The boundary element method for elasticity problems with concentrated loads based on displacement singular elements

Wei Zhou[1], Qiang Yue[1], Qiao Wang[1,2,*], Y.T. Feng[2], Xiaolin Chang[1]

[1]State Key Laboratory of Water Resources and Hydropower Engineering Science, Wuhan University, Wuhan 430072, China

[2] Zienkiewicz Centre for Computational Engineering, Swansea University, UK

Abstract

The boundary element method (BEM) has been implemented in elasticity problems very successfully because of its high accuracy. However, there are very few investigations about BEM with concentrated loads. The displacement at the concentrated load point is infinite and traditional elements will lead inaccurate results near the concentrated load point. This paper proposes two types of displacement singular elements to approximate the displacement near concentrated load point, and high accuracy can be obtained without refinement. The second type of displacement singular element is a general element type, which can work well for both problems with or without boundary concentrated loads. Numerical examples have been studied and compared with results obtained by traditional BEM and finite element method (FEM) to show the necessary of the proposed methods.

Keywords: boundary element method; elasticity problem; concentrated loads; displacement singular element.

1. Introduction

The boundary element method [1-6] has been applied in many areas [7-12] because of its high accuracy and boundary-only discretization. Compared with the finite element method (FEM), BEM can obtain very high accuracy with much fewer elements on the boundary.

In elasticity problems, most of the boundary conditions are displacements and surface tractions. BEM can impose these boundary conditions directly and it is more convenient than FEM. In some cases, there are concentrated loads needed to be imposed on the computed domain. In FEM, the concentrated loads can be treated as nodal forces. However, in BEM, the concentrated loads cannot be imposed on nodes directly because of the singularities and the detail can be found in section 2. Actually, this is not a serious problem since one can let the nodes do not coincide

with the concentrated load points. This treatment is reasonable because the displacement at the concentrated load point is infinite and its value can't be considered directly in numerical computation. However, the accuracy is low if using the traditional elements in BEM, especially at points near the concentrated loads. This is because the traditional elements cannot approximate the rapidly changed displacement efficiently. Using more elements near the concentrated loads may improve the accuracy but much more time would be cost. In fact, the same problem exists in FEM. In FEM, the results near the concentrated loads are also very inaccurate and much more elements are needed to obtain reasonable results.

Only a few literatures for BEM with concentrated loads in elasticity problems can be found. Qian [13] given the boundary integral equation for problems with concentrated loads based on Betti's reciprocity theorem, and the contribution of concentrated loads were not considered accurately since traditional elements were used. Wang et al. [14] proposed a spline boundary integral equation with concentrated forces, and two kinds of singularities were treated. However, the validity and accuracy of the method for dealing with singularities is needed to be proved further. This paper tries to consider the contribution of concentrated loads more accurately by using displacement singular elements. The main idea is constructing new shape functions by assuming the displacement is infinite at concentrated load points. Two types of singular elements are proposed, the firs type has only one concentrated load point, while the second type has two concentrated load points at the edges of the element. Both types of elements can obtain very high accuracy without refinement mesh. Especially, the second type element can also work well for problems without concentrated load points, thus, one can use it on the entire boundary without considering if there have boundary concentrated loads.

This paper is organized as follows. The boundary integral equation for elasticity problems with concentrated loads is introduced first. Then the displacement singular elements are proposed in section 3 and section 4, followed by the method for computing the singular and nearly singular integrals in section 5. Finally, numerical examples are tested to show the accuracy of the proposed methods.

2. Boundary integral equation for elasticity problems

To obtain the boundary integral equation (BIE) of elasticity problems with concentrated load, one can treat the concentrated load as the limit of body force. The traditional BIE with body force can be written as [15]:

$$c(\mathbf{x})\mathbf{u}(\mathbf{x}) = \int_{\Gamma} \mathbf{U}(\mathbf{x},\mathbf{y})\mathbf{t}(\mathbf{y})\mathrm{d}\Gamma(\mathbf{y}) - \int_{\Gamma} \mathbf{T}(\mathbf{x},\mathbf{y})\mathbf{u}(\mathbf{y})\mathrm{d}\Gamma(\mathbf{y}) + \int_{\Omega} \mathbf{U}(\mathbf{x},\mathbf{y})\mathbf{b}(\mathbf{y})\mathrm{d}\Omega(\mathbf{y}) \quad (1)$$

where Ω is the computed domain and Γ is the boundary. $\mathbf{x}$ and $\mathbf{y}$ are points in $\mathbb{R}^2$. $c(\mathbf{x})$ is a coefficient relative with the position of $\mathbf{x}$. $\mathbf{u}$ are the displacement, $\mathbf{t}$ are the tractions and $\mathbf{b}(y)$ are the body forces. $\mathbf{U}(\mathbf{x},\mathbf{y})$ and $\mathbf{T}(\mathbf{x},\mathbf{y})$ are the Kelvin kernels. For 2D plane strain problems, they can be written as

$$U_{ki}(\mathbf{x},\mathbf{y}) = \frac{-1}{8\pi(1-\nu)\mu}\{(3-4\nu)\ln(r)\delta_{ki} - r_{,k}r_{,i}\} \quad (2)$$

$$T_{ki}(\mathbf{x},\mathbf{y}) = \frac{-1}{4\pi(1-\nu)r}\{[(1-2\nu)\delta_{ki} + 2r_{,k}r_{,i}]\frac{\partial r}{\partial \mathbf{n}(\mathbf{y})} - (1-2\nu)(r_{,k}n_i(\mathbf{y}) - r_{,i}n_k(\mathbf{y}))\} \quad (3)$$

where $r = r(\mathbf{x},\mathbf{y})$ is the distance between point $\mathbf{x}$ and $\mathbf{y}$. $\mathbf{n}(\mathbf{y})$ is the unit outward normal at point $\mathbf{y}$. μ is the shear modulus and ν is the Poisson ratio of the solid.

Suppose there is a concentrated load $\mathbf{f}$ at point $\mathbf{z}$ (see Figure 1(a)), and $\mathbf{f}$ can be equivalent to uniform body force $\mathbf{p}$ on a small area Ω_ε centered at $\mathbf{z}$ with radius ε (see Figure 1(b)), then one can have

$$\mathbf{p} = \frac{2\mathbf{f}}{\varepsilon^2\alpha} \quad (4)$$

where α is the angle of the corner (see Figure 1(b)). Then the contribution of the concentrated load can be computed by domain integral as

$$\lim_{\varepsilon\to 0}\int_{\Omega_\varepsilon} \mathbf{U}(\mathbf{x},\mathbf{y})\frac{2\mathbf{f}}{\varepsilon^2\alpha}\mathrm{d}\Omega(\mathbf{y}) = \lim_{\varepsilon\to 0}\int_{\theta_1}^{\theta_2}\int_0^{\varepsilon} \mathbf{U}(\mathbf{x},\mathbf{y})\frac{2\mathbf{f}}{\varepsilon^2\alpha} r_\varepsilon \mathrm{d}r_\varepsilon \mathrm{d}\theta \quad (5)$$

where r_ε and θ are the local polar coordinates, and $\alpha = \theta_2 - \theta_1$, in which θ_1 and θ_2 are the degrees of the two edges of the corner.

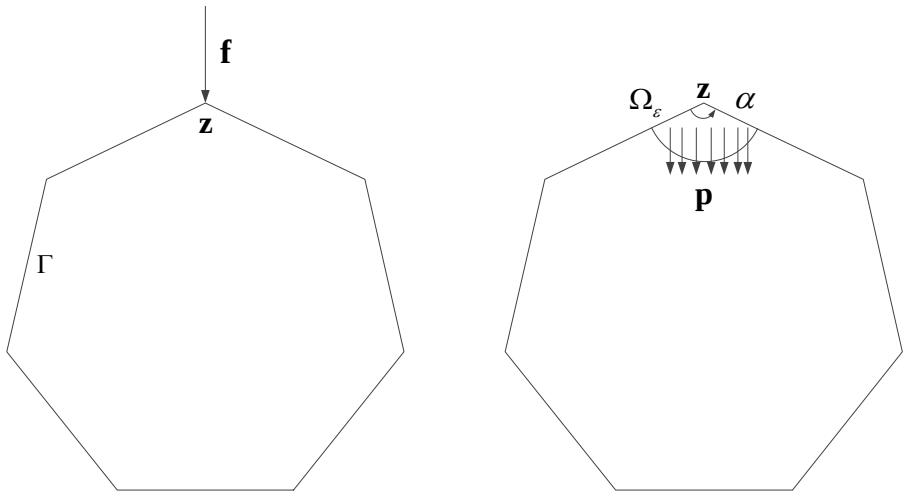

(a) (b)

Figure 1. Problem with concentrated load

The kernel $\mathbf{U}(\mathbf{x},\mathbf{y})$ can be expressed by Taylor's expansion at point $\mathbf{z}$ as

$$\begin{aligned}&\mathbf{U}(\mathbf{x},\mathbf{y})=\mathbf{U}(\mathbf{x},\mathbf{z})+r_\varepsilon\cos\theta\mathbf{U}_{,1}(\mathbf{x},\mathbf{z})+r_\varepsilon\sin\theta\mathbf{U}_{,2}(\mathbf{x},\mathbf{z})\\&+\frac{1}{2!}r_\varepsilon^2\cos^2\theta\mathbf{U}_{,11}(\mathbf{x},\mathbf{z})+\frac{2}{2!}r_\varepsilon^2\cos\theta\sin\theta\mathbf{U}_{,12}(\mathbf{x},\mathbf{z})+\frac{1}{2!}r_\varepsilon^2\sin^2\theta\mathbf{U}_{,22}(\mathbf{x},\mathbf{z})\\&+\mathbf{R}_n(\mathbf{x},\mathbf{y})\end{aligned}\tag{6}$$

where $\mathbf{R}_n(\mathbf{x},\mathbf{y})$ are the higher order expansions and

$$\mathbf{U}_{,i}(\mathbf{x},\mathbf{z})=\frac{\partial\mathbf{U}(\mathbf{x},\mathbf{y})}{\partial y_i}|_{\mathbf{y}=\mathbf{z}}\tag{7}$$

$$\mathbf{U}_{,ij}(\mathbf{x},\mathbf{z})=\frac{\partial\mathbf{U}^2(\mathbf{x},\mathbf{y})}{\partial y_i\partial y_j}|_{\mathbf{y}=\mathbf{z}}\tag{8}$$

The integral of the first term in Equation (6) can be computed as

$$\begin{aligned}&\lim_{\varepsilon\to0}\int_{\theta_1}^{\theta_2}\int_0^{\varepsilon}\mathbf{U}(\mathbf{x},\mathbf{z})\frac{2\mathbf{f}}{\varepsilon^2\alpha}r_\varepsilon\mathrm{d}r_\varepsilon\mathrm{d}\theta\\&=\lim_{\varepsilon\to0}\mathbf{U}(\mathbf{x},\mathbf{z})\frac{2\mathbf{f}}{\varepsilon^2\alpha}\int_{\theta_1}^{\theta_2}\int_0^{\varepsilon}r_\varepsilon\,\mathrm{d}r_\varepsilon\mathrm{d}\theta\\&=\lim_{\varepsilon\to0}\mathbf{U}(\mathbf{x},\mathbf{z})\mathbf{f}\\&=\mathbf{U}(\mathbf{x},\mathbf{z})\mathbf{f}\end{aligned}\tag{9}$$

The integral of the second term in Equation (6) can be computed as

$$\begin{aligned}&\lim_{\varepsilon\to0}\int_{\theta_1}^{\theta_2}\int_0^{\varepsilon}r_\varepsilon\cos\theta\mathbf{U}_{,1}(\mathbf{x},\mathbf{z})\frac{2\mathbf{f}}{\varepsilon^2\alpha}r_\varepsilon\mathrm{d}r_\varepsilon\mathrm{d}\theta\\&=\lim_{\varepsilon\to0}\mathbf{U}_{,1}(\mathbf{x},\mathbf{z})\frac{2\mathbf{f}}{\varepsilon^2\alpha}\int_{\theta_1}^{\theta_2}\int_0^{\varepsilon}r_\varepsilon^2\mathrm{d}r_\varepsilon\cos\theta\mathrm{d}\theta\\&=\lim_{\varepsilon\to0}\mathbf{U}_{,1}(\mathbf{x},\mathbf{z})\frac{2\varepsilon\mathbf{f}}{3\alpha}\int_{\theta_1}^{\theta_2}\cos\theta\mathrm{d}\theta\\&=0\end{aligned}\tag{10}$$

Similarly, the integrals of the rest terms in Equation (6) will be zero as $\varepsilon\to0$. Thus, Equation (5) will be

$$\lim_{\varepsilon\to0}\int_{\Omega_\varepsilon}\mathbf{U}(\mathbf{x},\mathbf{y})\frac{2\mathbf{f}}{\varepsilon^2\alpha}\mathrm{d}\Omega(\mathbf{y})=\mathbf{U}(\mathbf{x},\mathbf{z})\mathbf{f}\tag{11}$$

Suppose there are m concentrated loads on the boundary, the boundary integral equation (BIE) of elasticity problems without body force can be written as

$$c(\mathbf{x})\mathbf{u}(\mathbf{x})=\int_\Gamma\mathbf{U}(\mathbf{x},\mathbf{y})\mathbf{t}(\mathbf{y})\mathrm{d}\Gamma(\mathbf{y})-\int_\Gamma\mathbf{T}(\mathbf{x},\mathbf{y})\mathbf{u}(\mathbf{y})\mathrm{d}\Gamma(\mathbf{y})+\sum_{l=1}^{m}\mathbf{U}(\mathbf{x},\mathbf{z}_l)\mathbf{f}(\mathbf{z}_l)\tag{12}$$

where $\mathbf{f}(\mathbf{z}_l)$ is the concentrated load at point $\mathbf{z}_l$. It should be noted that $\mathbf{t}$ are regular values and the traction for the concentrated load points can be defined as

$$\mathbf{t}'(\mathbf{z}_l) = \mathbf{t}(\mathbf{z}_l) + \delta(\mathbf{y} - \mathbf{z}_l)\mathbf{f}(\mathbf{z}_l) \tag{13}$$

where $\delta(\mathbf{y} - \mathbf{z}_l)$ is the Dirac-delta function defined as

$$\delta(t) = \begin{cases} \infty & if \quad t = 0 \\ 0 & otherwise \end{cases} \tag{14}$$

Finally, one can obtain the matrix form by discretizing the boundary into elements as

$$\mathbf{A}\bar{\mathbf{u}} = \mathbf{B}\bar{\mathbf{t}} + \bar{\mathbf{B}}\mathbf{F} \tag{15}$$

where $\mathbf{A}$ and $\mathbf{B}$ are the coefficient matrices, and $\bar{\mathbf{u}}$ and $\bar{\mathbf{t}}$ are the vectors of nodal displacements and tractions on the boundary, and

$$\left[\bar{\mathbf{B}}\right]_{il} = \begin{bmatrix} U_{11}(\mathbf{x}_i, \mathbf{z}_l) & U_{12}(\mathbf{x}_i, \mathbf{z}_l) \\ U_{21}(\mathbf{x}_i, \mathbf{z}_l) & U_2(\mathbf{x}_i, \mathbf{z}_l) \end{bmatrix} \tag{16}$$

$$\mathbf{F} = \begin{bmatrix} f_1(\mathbf{z}_1) & f_2(\mathbf{z}_1) & \cdots & f_1(\mathbf{z}_m) & f_2(\mathbf{z}_m) \end{bmatrix}^{\mathrm{T}} \tag{17}$$

Equation (12) can also be obtained from the Betti's reciprocity theorem [13].

3. Displacement singular element with one concentrated load point

From the fundamental solution shown in Equation (2), one can indicate that the singular order of displacement at concentrated load point is $O(\ln(1/r))$, i.e. the displacement field is singular at the concentrated load point. Thus, the traditional shape function cannot approximate the displacement very well. To overcome this problem, displacement singular elements with kernel $\ln(1/r)$ can be proposed to approximate the displacement field more accurately, where r is the distance between the interested point and the concentrated force point.

3.1 Displacement Singular Element of Type One with Two Nodes (DSET1N2)

Now assuming the displacement in the singular element can be approximated by

$$u_i(\mathbf{y}) = \tilde{a}_i \ln\left(\frac{1}{|\mathbf{y} - \mathbf{z}|}\right) + \tilde{b}_i \tag{18}$$

where $i = 1, 2$ and $\mathbf{z}$ is the singular point, i.e. the concentrated force point. $\tilde{a}_i$ and $\tilde{b}_i$ are unknown coefficients.

Then suppose there are two nodes $\mathbf{y}_j, j = 1, 2$ in the element, where $\mathbf{y}_j \neq \mathbf{z}$ (see Figure 2). One can have

$$u_i(\mathbf{y}_1) = \tilde{a}_i \ln(\frac{1}{|\mathbf{y}_1 - \mathbf{z}|}) + \tilde{b}_i \tag{19}$$

$$u_i(\mathbf{y}_2) = \tilde{a}_i \ln(\frac{1}{|\mathbf{y}_2 - \mathbf{z}|}) + \tilde{b}_i \tag{20}$$

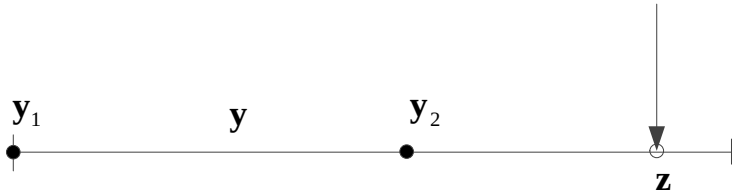

Figure 2. Singular element with two nodes

From Equations (19) and (20), one can obtain

$$\tilde{a}_i = \frac{u_i(\mathbf{y}_1) - u_i(\mathbf{y}_2)}{\ln(1/|\mathbf{y}_1 - \mathbf{z}|) - \ln(1/|\mathbf{y}_2 - \mathbf{z}|)} \tag{21}$$

$$\tilde{b}_i = \frac{u_i(\mathbf{y}_1)\ln(1/|\mathbf{y}_2 - \mathbf{z}|) - u_i(\mathbf{y}_2)\ln(1/|\mathbf{y}_1 - \mathbf{z}|)}{\ln(1/|\mathbf{y}_2 - \mathbf{z}|) - \ln(1/|\mathbf{y}_1 - \mathbf{z}|)} \tag{22}$$

Then the displacement can be rewritten as

$$u_i(\mathbf{y}) = \sum_{j=1}^{2} \phi_j(\mathbf{y}) u_i(\mathbf{y}_j) \tag{23}$$

where $\phi_j(\mathbf{y})$ are shape functions:

$$\phi_1(\mathbf{y}) = \frac{\ln(1/|\mathbf{y} - \mathbf{z}|) - \ln(1/|\mathbf{y}_2 - \mathbf{z}|)}{\ln(1/|\mathbf{y}_1 - \mathbf{z}|) - \ln(1/|\mathbf{y}_2 - \mathbf{z}|)} \tag{24}$$

$$\phi_2(\mathbf{y}) = -\frac{\ln(1/|\mathbf{y} - \mathbf{z}|) - \ln(1/|\mathbf{y}_1 - \mathbf{z}|)}{\ln(1/|\mathbf{y}_1 - \mathbf{z}|) - \ln(1/|\mathbf{y}_2 - \mathbf{z}|)} \tag{25}$$

Using this singular element, the concentrated load can be imposed accurately, and no refinement is needed near the concentrated load point. The procedure to create the singular elements is described as below.

Step 1: Create the boundary element edges. Each boundary element contains two end points (see Figure 2). This procedure is the same as in traditional BEM.

Step 2: Compute the distances between concentrated load point $\mathbf{z}$ and two end points for each element. If both the distances are less than a prescribed value, this element is considered as singular element (see Figure 3). In this paper, the prescribed value is $2.5l$, where l is the length of the element.

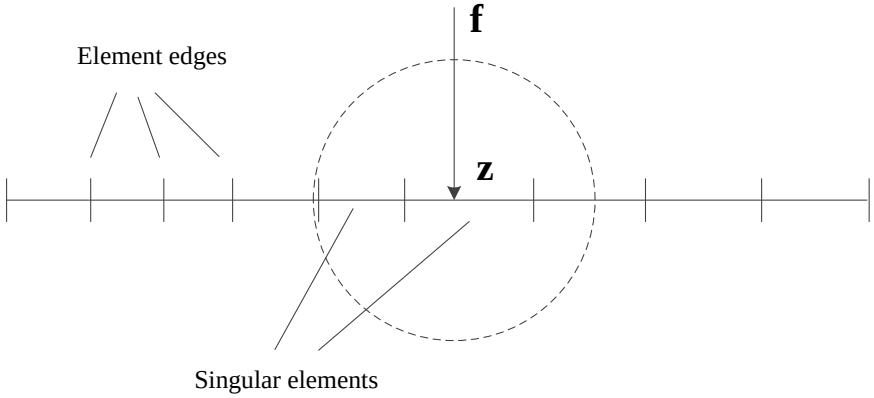

Figure 3. Find out singular elements.

Step 3: Create the singular element. Suppose the local coordinates of the element is from -1 to 1, and the local coordinate ξ_0 of the concentrated load point in this element can be obtained. Then the local coordinates ξ_i of the nodes can be defined as:

(i) $\xi_1 = -1.0$, $\xi_2 = 0.25$, if $0.5 < \xi_0 \le 1.0$

(ii) $\xi_1 = -1.0$, $\xi_2 = -0.25$, if $0 < \xi_0 \le 0.5$

(iii) $\xi_1 = 0.25$, $\xi_2 = 1.0$, if $-0.5 < \xi_0 \le 0$

(iv) $\xi_1 = -0.25$, $\xi_2 = 1.0$, if $-1.0 \le \xi_0 < -0.5$

(v) $\xi_1 = -1.0$, $\xi_2 = 1.0$, if the concentrated load point is not in this element.

Step 4: Create the traditional element. This procedure is the same as in the traditional BEM.

If assuming the concentrated load point is at one of the edges of the singular elements, and using discontinue element, then the local coordinates ξ_i of the nodes can be defined as $\xi_1 = -0.25$ and $\xi_2 = 0.25$. This type of singular elements can be called displacement singular element of type one with two nodes (DSET1N2). At last, one can apply Equation (15) to solve the problem. In Equation (15), the corresponding coefficient matrix $\mathbf{B}$ can also be computed by the displacement singular elements like coefficient matrix $\mathbf{A}$, or it can be computed by traditional elements.

3.2 Displacement Singular Element of Type One with Three Nodes (DSET1N3)

Similarly, one can create higher order elements with three nodes by assuming

$$u_i(\mathbf{y}) = \bar{a}_i \ln\left(\frac{1}{|\mathbf{y}-\mathbf{z}|}\right) + \bar{b}_i \xi + \bar{c}_i \tag{26}$$

where $\bar{a}_i$, $\bar{b}_i$ and $\bar{c}_i$ are unknown coefficients, ξ is the local coordinate of point $\mathbf{y}$. The shape functions are defined as

$$\phi_1(\mathbf{y})=\frac{(\xi_3-\xi_2)\ln(|\mathbf{y}-\mathbf{z}|)+[\ln(|\mathbf{y}_2-\mathbf{z}|)-\ln(|\mathbf{y}_3-\mathbf{z}|)]\xi+\ln(|\mathbf{y}_3-\mathbf{z}|)\xi_2-\ln(|\mathbf{y}_2-\mathbf{z}|)\xi_3}{\ln(|\mathbf{y}_1-\mathbf{z}|)(\xi_3-\xi_2)+\ln(|\mathbf{y}_2-\mathbf{z}|)(\xi_1-\xi_3)+\ln(|\mathbf{y}_3-\mathbf{z}|)(\xi_2-\xi_1)} \tag{27}$$

$$\phi_2(\mathbf{y})=\frac{(\xi_1-\xi_3)\ln(|\mathbf{y}-\mathbf{z}|)+[\ln(|\mathbf{y}_3-\mathbf{z}|)-\ln(|\mathbf{y}_1-\mathbf{z}|)]\xi+\ln(|\mathbf{y}_1-\mathbf{z}|)\xi_3-\ln(|\mathbf{y}_3-\mathbf{z}|)\xi_1}{\ln(|\mathbf{y}_1-\mathbf{z}|)(\xi_3-\xi_2)+\ln(|\mathbf{y}_2-\mathbf{z}|)(\xi_1-\xi_3)+\ln(|\mathbf{y}_3-\mathbf{z}|)(\xi_2-\xi_1)} \tag{28}$$

$$\phi_3(\mathbf{y})=\frac{(\xi_2-\xi_1)\ln(|\mathbf{y}-\mathbf{z}|)+[\ln(|\mathbf{y}_1-\mathbf{z}|)-\ln(|\mathbf{y}_2-\mathbf{z}|)]\xi+\ln(|\mathbf{y}_2-\mathbf{z}|)\xi_1-\ln(|\mathbf{y}_1-\mathbf{z}|)\xi_2}{\ln(|\mathbf{y}_1-\mathbf{z}|)(\xi_3-\xi_2)+\ln(|\mathbf{y}_2-\mathbf{z}|)(\xi_1-\xi_3)+\ln(|\mathbf{y}_3-\mathbf{z}|)(\xi_2-\xi_1)} \tag{29}$$

where ξ_i is local coordinates of the *i*th nodes, $i=1,2,3$. This type of singular element can be called displacement singular element of type one with three nodes (DSET1N3).

One can check the values of the shape functions by

$$\sum_{j=1}^{n}\phi_j(\mathbf{y})=1 \tag{30}$$

and

$$\phi_j(\mathbf{y}_i)=\delta_{ij}=\begin{cases}1, & i=j\\ 0, & i\neq j\end{cases} \tag{31}$$

where n is the total number of nodes in each element, and $\mathbf{y}\neq\mathbf{z}$.

4. Displacement singular element with two concentrated load points

Displacement singular element of type one only suitable for at most one concentrated load point on each element. In this section, a general type of element with two concentrated load points is defined.

4.1 Displacement Singular Element of Type Two with Three Nodes (DSET2N3)

Suppose the concentrated load points are at the edges, then a singular element with three nodes can be defined as Figure 4, and the displacement can be approximated by

$$u_i(\mathbf{y})=\hat{a}_i\ln(\frac{1}{|\mathbf{y}-\mathbf{z}_1|})+\hat{b}_i\ln(\frac{1}{|\mathbf{y}-\mathbf{z}_2|})+\hat{c}_i \tag{32}$$

where $\mathbf{z}_1$ and $\mathbf{z}_2$ are concentrated load points, $\hat{a}_i$, $\hat{b}_i$ and $\hat{c}_i$ are unknown coefficients.

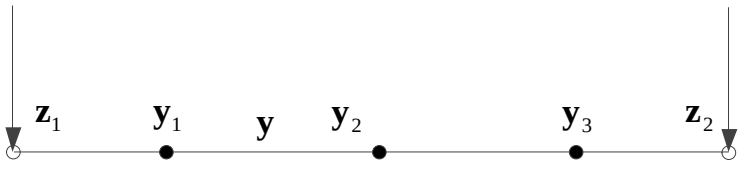

Figure 4. Displacement singular element of type two with three nodes (DSET2N3)

At last, one can have

$$u_i(\mathbf{y})=\sum_{j=1}^{3}\phi_j(\mathbf{y})u_i(\mathbf{y}_j) \tag{33}$$

where

$$\phi_1(\mathbf{y}) = \frac{1}{C}\{\ln(\frac{|\mathbf{y}_3 - \mathbf{z}_2|}{|\mathbf{y}_2 - \mathbf{z}_2|})\ln(\frac{|\mathbf{y}_3 - \mathbf{z}_1|}{|\mathbf{y} - \mathbf{z}_1|}) - \ln(\frac{|\mathbf{y}_3 - \mathbf{z}_1|}{|\mathbf{y}_2 - \mathbf{z}_1|})\ln(\frac{|\mathbf{y}_3 - \mathbf{z}_2|}{|\mathbf{y} - \mathbf{z}_2|})\} \tag{34}$$

$$\phi_2(\mathbf{y}) = \frac{1}{C}\{\ln(\frac{|\mathbf{y}_1 - \mathbf{z}_2|}{|\mathbf{y}_3 - \mathbf{z}_2|})\ln(\frac{|\mathbf{y}_1 - \mathbf{z}_1|}{|\mathbf{y} - \mathbf{z}_1|}) - \ln(\frac{|\mathbf{y}_1 - \mathbf{z}_1|}{|\mathbf{y}_3 - \mathbf{z}_1|})\ln(\frac{|\mathbf{y}_1 - \mathbf{z}_2|}{|\mathbf{y} - \mathbf{z}_2|})\} \tag{35}$$

$$\phi_3(\mathbf{y}) = \frac{1}{C}\{\ln(\frac{|\mathbf{y}_1 - \mathbf{z}_1|}{|\mathbf{y}_2 - \mathbf{z}_1|})\ln(\frac{|\mathbf{y}_1 - \mathbf{z}_2|}{|\mathbf{y} - \mathbf{z}_2|}) - \ln(\frac{|\mathbf{y}_1 - \mathbf{z}_2|}{|\mathbf{y}_2 - \mathbf{z}_2|})\ln(\frac{|\mathbf{y}_1 - \mathbf{z}_1|}{|\mathbf{y} - \mathbf{z}_1|})\} \tag{36}$$

$$C = \ln(\frac{|\mathbf{y}_3 - \mathbf{z}_1|}{|\mathbf{y}_1 - \mathbf{z}_1|})\ln(\frac{|\mathbf{y}_3 - \mathbf{z}_2|}{|\mathbf{y}_2 - \mathbf{z}_2|}) - \ln(\frac{|\mathbf{y}_3 - \mathbf{z}_1|}{|\mathbf{y}_2 - \mathbf{z}_1|})\ln(\frac{|\mathbf{y}_3 - \mathbf{z}_2|}{|\mathbf{y}_1 - \mathbf{z}_2|}) \tag{37}$$

This type of element can be called displacement singular element of type two with three nodes (DSET2N3).

4.2 Displacement Singular Element of Type Two with Four Nodes (DSET2N4)

To obtain higher accuracy, one can create displacement singular element of type two with four nodes (DSET2N4) by assuming

$$u_i(\mathbf{y}) = \hat{a}_i \ln(\frac{1}{|\mathbf{y} - \mathbf{z}_1|}) + \hat{b}_i \ln(\frac{1}{|\mathbf{y} - \mathbf{z}_2|}) + \hat{c}_i\xi + \hat{d}_i \tag{38}$$

where $\hat{a}_i$, $\hat{b}_i$, $\hat{c}_i$ and $\hat{d}_i$ are unknown coefficients. At last, one can obtain the shape functions as

$$\phi_i(\mathbf{y}) = a_i \ln(\frac{1}{|\mathbf{y} - \mathbf{z}_1|}) + b_i \ln(\frac{1}{|\mathbf{y} - \mathbf{z}_2|}) + c_i\xi + d_i, \quad i = 1,2,3,4 \tag{39}$$

where

$$d_1 = 1 - a_1 \ln(\frac{1}{|\mathbf{y}_1 - \mathbf{z}_1|}) - b_1 \ln(\frac{1}{|\mathbf{y}_1 - \mathbf{z}_2|}) - c_1\xi_1 \tag{40}$$

$$d_i = -a_i \ln(\frac{1}{|\mathbf{y}_1 - \mathbf{z}_1|}) - b_i \ln(\frac{1}{|\mathbf{y}_1 - \mathbf{z}_2|}) - c_i\xi_1, \quad i = 2,3,4 \tag{41}$$

$$c_1 = \frac{1}{\xi_1 - \xi_4}[1 - a_1 \ln(\frac{|\mathbf{y}_4 - \mathbf{z}_1|}{|\mathbf{y}_1 - \mathbf{z}_1|}) - b_1 \ln(\frac{|\mathbf{y}_4 - \mathbf{z}_2|}{|\mathbf{y}_1 - \mathbf{z}_2|})] \tag{42}$$

$$c_i = \frac{1}{\xi_1 - \xi_4}[-a_i \ln(\frac{|\mathbf{y}_4 - \mathbf{z}_1|}{|\mathbf{y}_1 - \mathbf{z}_1|}) - b_i \ln(\frac{|\mathbf{y}_4 - \mathbf{z}_2|}{|\mathbf{y}_1 - \mathbf{z}_2|})], \quad i = 2,3 \tag{43}$$

$$c_4 = \frac{1}{\xi_1 - \xi_4}[-1 - a_4 \ln(\frac{|\mathbf{y}_4 - \mathbf{z}_1|}{|\mathbf{y}_1 - \mathbf{z}_1|}) - b_4 \ln(\frac{|\mathbf{y}_4 - \mathbf{z}_2|}{|\mathbf{y}_1 - \mathbf{z}_2|})] \tag{44}$$

$$b_1 = \frac{(\xi_3 - \xi_4)A_2}{B_1 A_2 - B_2 A_1} \tag{45}$$

$$b_2 = \frac{(\xi_4 - \xi_3)A_1}{B_1 A_2 - B_2 A_1} \tag{46}$$

$$b_3 = \frac{(\xi_2 - \xi_4)A_1 - (\xi_1 - \xi_4)A_2}{B_1 A_2 - B_2 A_1} \tag{47}$$

$$b_4 = \frac{(\xi_1 - \xi_3)A_2 + (\xi_3 - \xi_2)A_1}{B_1 A_2 - B_2 A_1} \tag{48}$$

$$a_1 = \frac{(\xi_3 - \xi_4)B_2}{A_1 B_2 - A_2 B_1} \tag{49}$$

$$a_2 = \frac{(\xi_4 - \xi_3)B_1}{A_1 B_2 - A_2 B_1} \tag{50}$$

$$a_3 = \frac{(\xi_2 - \xi_4)B_1 - (\xi_1 - \xi_4)B_2}{A_1 B_2 - A_2 B_1} \tag{51}$$

$$a_4 = \frac{(\xi_1 - \xi_3)B_2 + (\xi_3 - \xi_2)B_1}{A_1 B_2 - A_2 B_1} \tag{52}$$

$$A_1 = \ln(\frac{|\mathbf{y}_4 - \mathbf{z}_1|}{|\mathbf{y}_1 - \mathbf{z}_1|})(\xi_3 - \xi_4) - \ln(\frac{|\mathbf{y}_4 - \mathbf{z}_1|}{|\mathbf{y}_3 - \mathbf{z}_1|})(\xi_1 - \xi_4) \tag{53}$$

$$B_1 = \ln(\frac{|\mathbf{y}_4 - \mathbf{z}_2|}{|\mathbf{y}_1 - \mathbf{z}_2|})(\xi_3 - \xi_4) - \ln(\frac{|\mathbf{y}_4 - \mathbf{z}_2|}{|\mathbf{y}_3 - \mathbf{z}_2|})(\xi_1 - \xi_4) \tag{54}$$

$$A_2 = \ln(\frac{|\mathbf{y}_4 - \mathbf{z}_1|}{|\mathbf{y}_2 - \mathbf{z}_1|})(\xi_3 - \xi_4) - \ln(\frac{|\mathbf{y}_4 - \mathbf{z}_1|}{|\mathbf{y}_3 - \mathbf{z}_1|})(\xi_2 - \xi_4) \tag{55}$$

$$B_2 = \ln(\frac{|\mathbf{y}_4 - \mathbf{z}_2|}{|\mathbf{y}_2 - \mathbf{z}_2|})(\xi_3 - \xi_4) - \ln(\frac{|\mathbf{y}_4 - \mathbf{z}_2|}{|\mathbf{y}_3 - \mathbf{z}_2|})(\xi_2 - \xi_4) \tag{56}$$

One should note that the displacement singular elements can also be used for case without concentrated load, especially for displacement singular elements of type two (DSET2). If using DSET2 to discretize the whole boundary, one does not need to care about where the boundary concentrated load located while meshing, and only the equivalent concentrated loads at the nearest

element edges are needed to be computed.

One can find out that element type DSET2 also satisfies Equations (30) and (31).

5. Computation of the singular integrals

In the displacement singular element, the shape functions have singular kernels and the integral should be dealt with carefully. Take the DSET2N3 as example, one may need to compute integrals with two singular kernels like

$$\int_{\Gamma} \mathbf{U}(\mathbf{x},\mathbf{y})[\hat{a}_i \ln(\frac{1}{|\mathbf{y}-\mathbf{z}_1|}) + \hat{b}_i \ln(\frac{1}{|\mathbf{y}-\mathbf{z}_2|})]d\Gamma(\mathbf{y}) \tag{57}$$

or

$$\int_{\Gamma} \mathbf{T}(\mathbf{x},\mathbf{y})[\hat{a}_i \ln(\frac{1}{|\mathbf{y}-\mathbf{z}_1|}) + \hat{b}_i \ln(\frac{1}{|\mathbf{y}-\mathbf{z}_2|})]d\Gamma(\mathbf{y}) \tag{58}$$

For a given element, the integrals can be classified into three types (see Figure 5): (i) Regular-singular integrals; (ii) Nearly singular-singular integrals; and (iii) Singular-singular integrals.

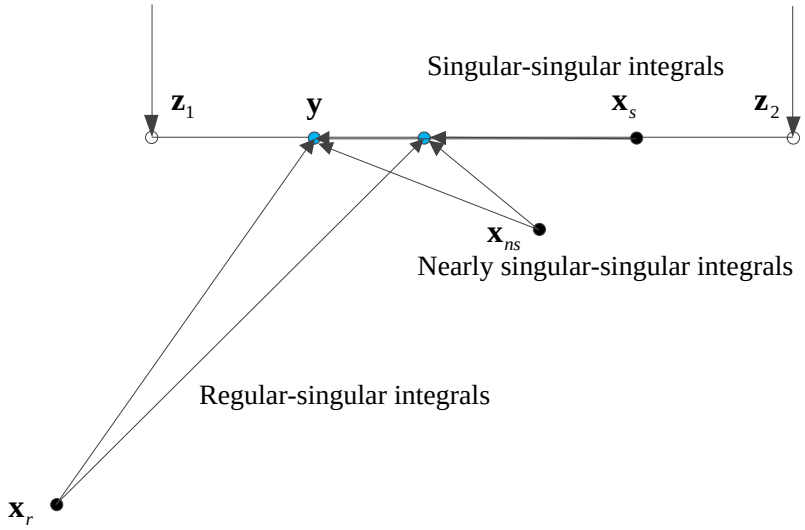

Figure 5. Integrals on each element

5.1. The regular-singular integrals

Suppose the distance between nodes $\mathbf{x}$ and the center of element is l_0, if $l_0 \geq 4l$, then the integrals can be considered as regular-singular integrals (see $\mathbf{x}_r$ in Figure 5). It only has weakly singular integrals in this case. However, there are two singular points at the edges of element; thus, one can subdivide the element into two segments at the center, and there is only one singular point on each segment. As shown in Figure 6, $\mathbf{z}_1$ is still the singular point, and $\mathbf{z}_2$ becomes the nearly singular point. To compute the nearly singular integrals caused by $\mathbf{z}_2$ accurately, this

segment can further be subdivided into sub-segments adaptively. Finally, there are two types of segments left, one type contains singular point $\mathbf{z}_1$, which is also far away from point $\mathbf{z}_2$ and can be computed by self-adaptive coordinate transformation method [16]. The other segments have only regular integrals since they are far away from both $\mathbf{z}_1$ and $\mathbf{z}_2$.

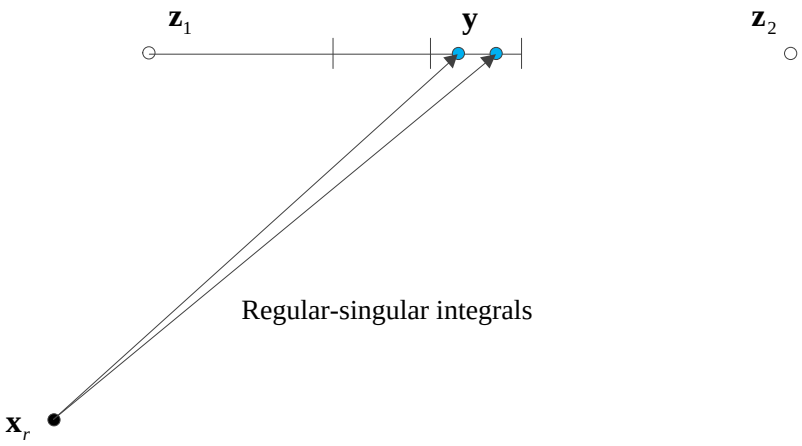

Figure 6. Subdivision for regular-singular integrals

5.2. The nearly singular-singular integrals

If $l_0 < 4l$ and point $\mathbf{x}$ is not on the element, then the integral can be considered as nearly singular-singular integral (see point $\mathbf{x}_{ns}$ in Figure 5). Subdividing the element adaptively as done for the regular-singular integrals, one can finally obtain two types of integrals, i.e. weakly singular integrals with one singular point and regular integrals with no singular or nearly singular point.

5.3. The singular-singular integrals

If point $\mathbf{x}$ is on the element, the integral can be considered as singular-singular integral (see point $\mathbf{x}_s$ in Figure 5). To compute this integral accurately, the element can be subdivided into three segments $\mathbf{z}_1\mathbf{s}_1$, $\mathbf{s}_1\mathbf{s}_2$ and $\mathbf{s}_2\mathbf{z}_2$ (see Figure 7(a)), where $\mathbf{s}_1$ is the middle point between $\mathbf{z}_1$ and $\mathbf{x}_s$, and $\mathbf{s}_2$ is the middle point between $\mathbf{z}_2$ and $\mathbf{x}_s$.

For segment $\mathbf{z}_1\mathbf{s}_1$, the integral is a weakly singular integral, in which $\mathbf{z}_1$ is the singular point, and $\mathbf{x}_s$ and $\mathbf{z}_2$ are the nearly singular points. Thus, this integral can be computed accurately by the adaptive subdivision scheme as used in the regular-singular integrals and the nearly singular-singular integrals. Segment $\mathbf{s}_S\mathbf{z}_2$ can be handled using the same way.

For segment $\mathbf{s}_1\mathbf{s}_2$, the integral is a weakly singular integral or strongly singular integral, in which $\mathbf{x}_s$ is the singular points, and $\mathbf{z}_1$ and $\mathbf{z}_2$ are the nearly singular points. Then segment $\mathbf{s}_1\mathbf{s}_2$ can be subdivided into three sub-segments $\mathbf{s}_1\mathbf{s}_3$, $\mathbf{s}_3\mathbf{s}_4$ and $\mathbf{s}_4\mathbf{s}_2$ (see Figure 7(b)).

Segments $\mathbf{s}_1\mathbf{s}_3$ and $\mathbf{s}_4\mathbf{s}_2$ have only nearly singular integrals with nearly singular points $\mathbf{z}_1$, $\mathbf{z}_2$ and $\mathbf{x}_s$, which can use the adaptive subdivision scheme to obtain the regular integrals. Keep subdivision segment $\mathbf{s}_3\mathbf{s}_4$ into three sub-segments like this way, until the middle segment which contains the singular point $\mathbf{x}_s$ is far away from points $\mathbf{z}_1$ and $\mathbf{z}_2$, and the integral on this segment can be computed by self-adaptive coordinate transformation method [16] for weakly singular kernel, or by singularity subtraction method [17, 18] for strongly singular kernel. However, one should note that the rigid body motion method is still valid and it is applied in this paper to compute the strongly singular integrals in Equation (58).

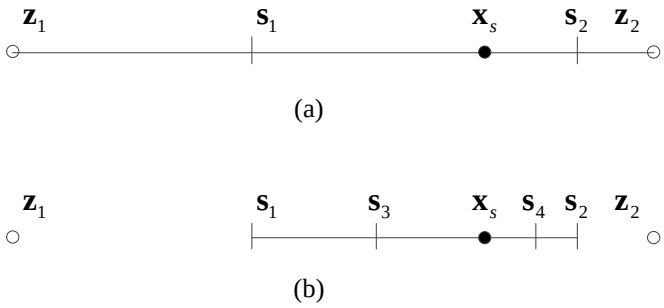

Figure 7. Subdivision for singular-singular integrals

6. Numerical examples

Numerical examples have been studied in this section to verify the accuracy of the proposed methods. For the purpose of error estimation, a formula is defined as

$$e = \sqrt{(\sum_{i=1}^{N}(u_i^{(e)} - u_i^{(n)})^2) / (\sum_{i=1}^{N}(u_i^{(e)})^2)} \tag{59}$$

where $u_i^{(e)}$ and $u_i^{(n)}$ refer to the exact and numerical solutions, respectively. In all the examples, the Young's modulus $E = 1.0$ and Poisson's ratio $\nu = 0.25$.

6.1. Lame problem

In this example, a hollow cylinder under uniform pressure on the inner surface shown in Figure 8 is studied to verify the displacement singular elements. The problem is a plane strain problem and only a quarter of the geometry can be analyzed due to the symmetry of the problem (see Figure 8(b)).

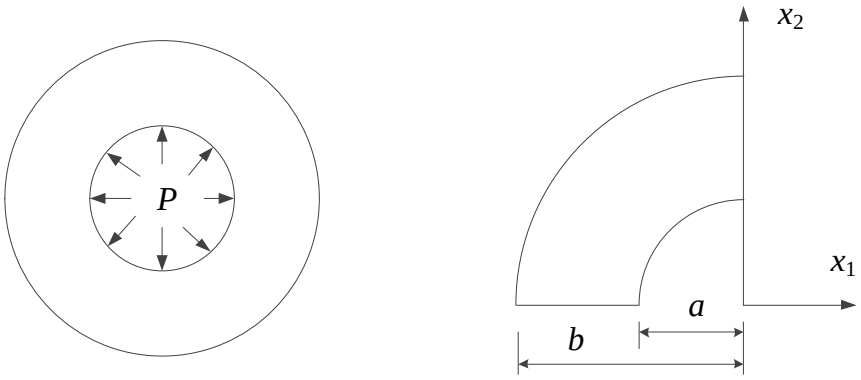

(a) (b)

Figure 8. Lame problem

The analytical solutions for the displacements and stresses are given as [15]

$$u_1 = \frac{1}{2\mu}\frac{Pa^2 r}{b^2 - a^2}[(1-2\nu) + \frac{b^2}{r^2}]\cos\theta, \tag{60}$$

$$u_2 = \frac{1}{2\mu}\frac{Pa^2 r}{b^2 - a^2}[(1-2\nu) + \frac{b^2}{r^2}]\sin\theta. \tag{61}$$

$$\sigma_1 = \frac{a^2 p}{b^2 - a^2}(1 - \frac{b^2}{r^2}\cos 2\theta) \tag{62}$$

$$\sigma_2 = \frac{a^2 p}{b^2 - a^2}(1 + \frac{b^2}{r^2}\cos 2\theta) \tag{63}$$

$$\tau = -\frac{a^2 p}{b^2 - a^2}\frac{b^2}{r^2}\sin 2\theta \tag{64}$$

In this example, $a = 1$, $b = 2$ and $P = 1$. DSET2N3 and DSET2N4 are applied to discretize the boundary. The relative errors computed from 153 points for the displacements and stresses are shown in Figures 9 and 10. It can be observed that both element types can obtain good results for traditional problem without concentrated load, and the accuracy obtained by DSET2N4 is much higher than it obtained by DSET2N3.

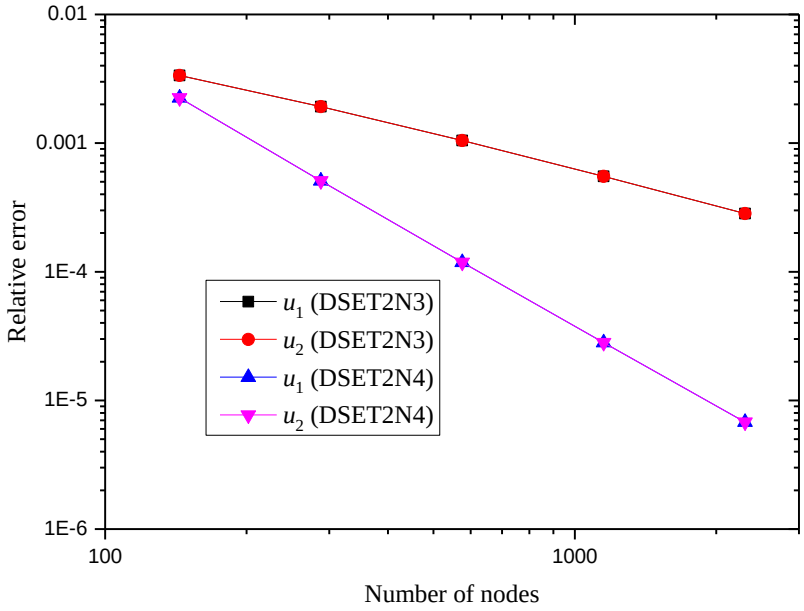

Figure 9. Relative of the displacements for Lame problem

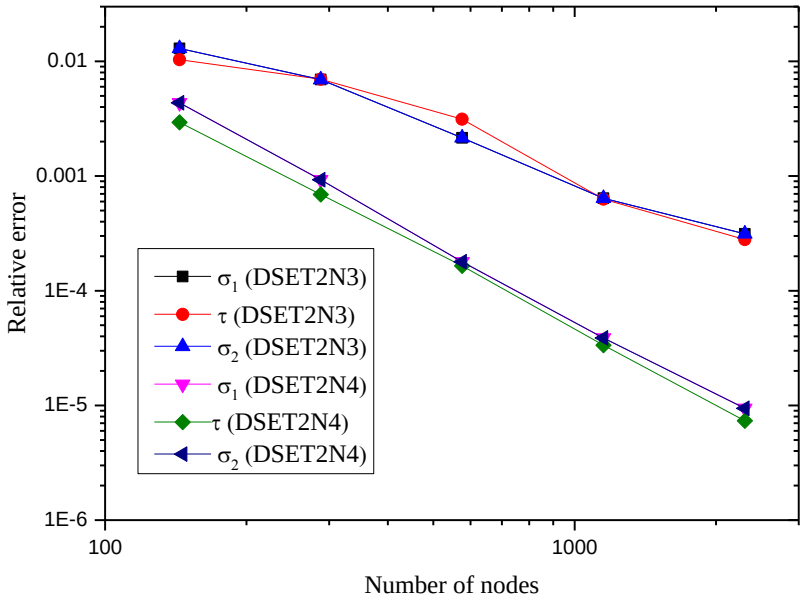

Figure 10. Relative of the stresses for Lame problem

6.2. Disk under compression by concentrated radial forces

A disk under compression is shown in Figure 11. The radius $R=5.0$, and the concentrated force $F=1$. The problem is considered as plane stress problem, and the analytic solutions of stresses are [19]

$$\sigma_1 = \frac{F}{\pi R}\left(1 - \frac{16R^2}{4R^2 - 4x_1^2}\right) \tag{65}$$

$$\sigma_2 = \frac{F}{\pi R} \tag{66}$$

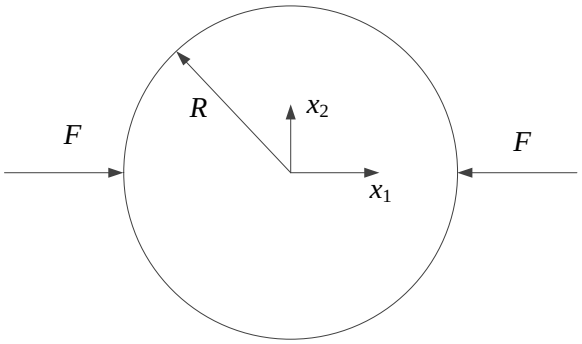

Figure 11. A disk under compression

The problem is solved by BEM with six types of elements: traditional discontinue linear elements with 2 nodes (Linear2), traditional discontinue quad elements with 3 nodes (Quad3), DSET1N2, DSET1N3, DSET2N3, DSET2N4. In the methods used DSET1N2 or DSET1N3, only DSET1N2 or DSET1N3 are applied for the elements near the concentrated force points, while Linear2 or Quad3 are applied for the rest elements. Since this example only has concentrated load boundary conditions, the final coefficient matrix is singular and the singular value decomposition is applied to solve the final system of equations. In all the methods, 480 nodes are used on the boundary, and the results of stresses on line $x_2 = 0$ can be observed in Figures 12, 13, 14 and 15. Accurate results can be obtained by BEM with DSET1N2, DSET1N3, DSET2N3 and DSET2N4, for both points near and far from the concentrated force points. However, the results obtained by BEM with Linear2 and Quad3 have huge errors for points near the concentrated force points.

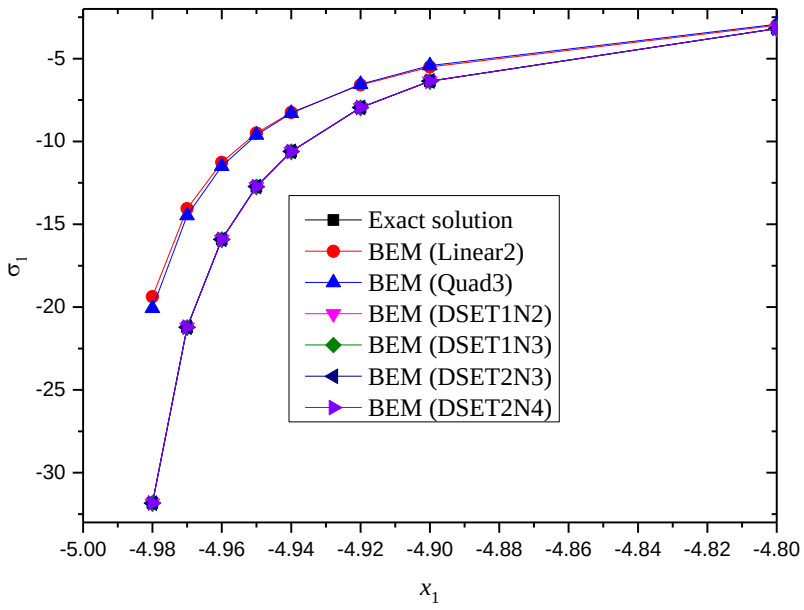

Figure 12. Stress σ_1 at points near the boundary

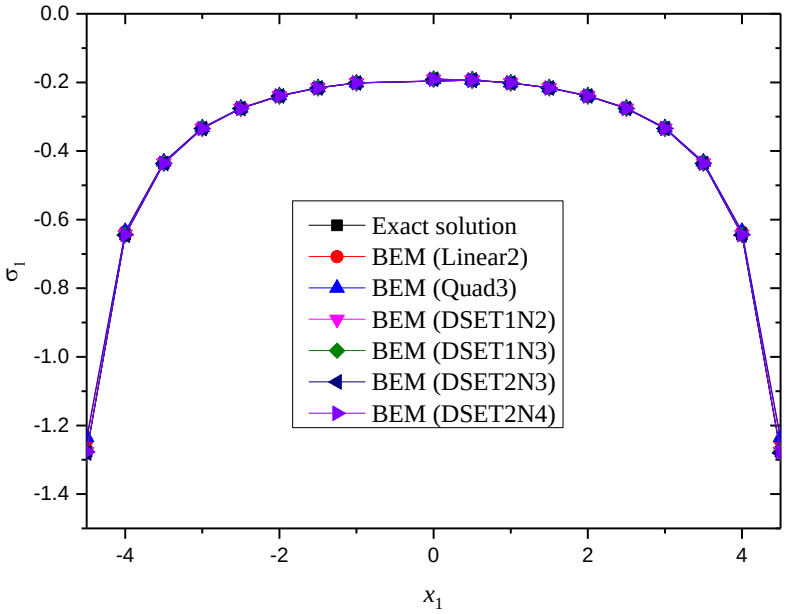

Figure 13. Stress σ_1 at points far from the boundary

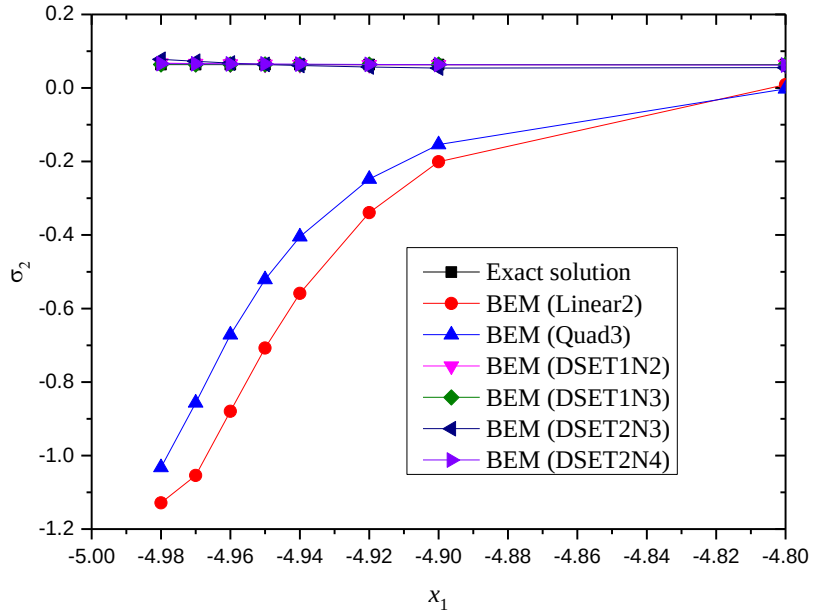

Figure 14. Stress σ_2 at points near the boundary

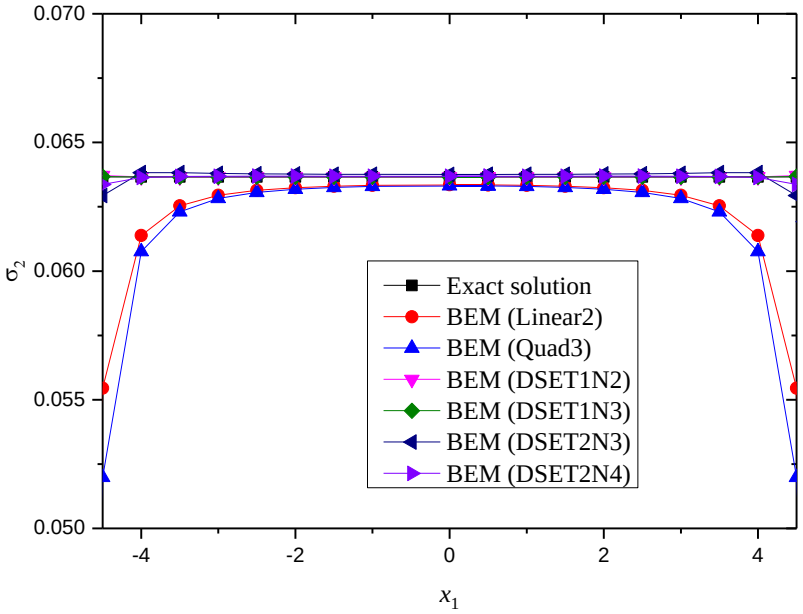

Figure 15. Stress σ_2 at points far from the boundary

6.3. A clamped beam under concentrated load

A clamped beam under concentrated load at the middle point is shown in Figure 16, and $L=4$, $H=2$, $F=1$. Six types of elements applied in example 6.2 are used to solve this

problem by BEM, and 288 nodes are used to discretize the boundary. For the purpose of comparison, finite element method (FEM) is also applied to solve the problem. The results of stresses on line $x_1 = 0$ are shown in Figures 17, 18, 19 and 20, and the results of displacement u_2 are shown in Figures 21 and 22. It can be observed that the results at points far from the concentrated load point are close to each other; however, the results at points near the concentrated load point have much difference. Actually, from Figures 18, 20 and 22, one can find out that the results obtained by BEM with DSET1N2, DSET1N3, DSET2N3 and DSET2N4 are in good agreement with each other. For stress σ_1, the results obtained by FEM with 320,000 elements also agrees well with BEM with displacement singular elements, however, the results obtained by other methods have much difference. For stress σ_2, the results obtained by BEM with displacement singular elements is highest, while the those obtained by BEM with traditional elements is lowest. For displacement u_2, the results obtained by FEM with 80,000 element has oscillation, and the values of u_2 obtained by BEM with displacement singular element are between those obtained by FEM with 320,000 elements and BEM with traditional elements.

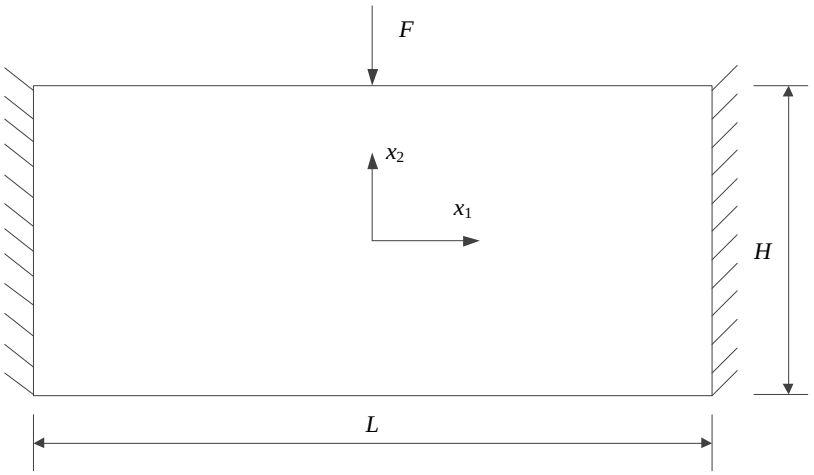

Figure 16. Clamped beam under concentrated load

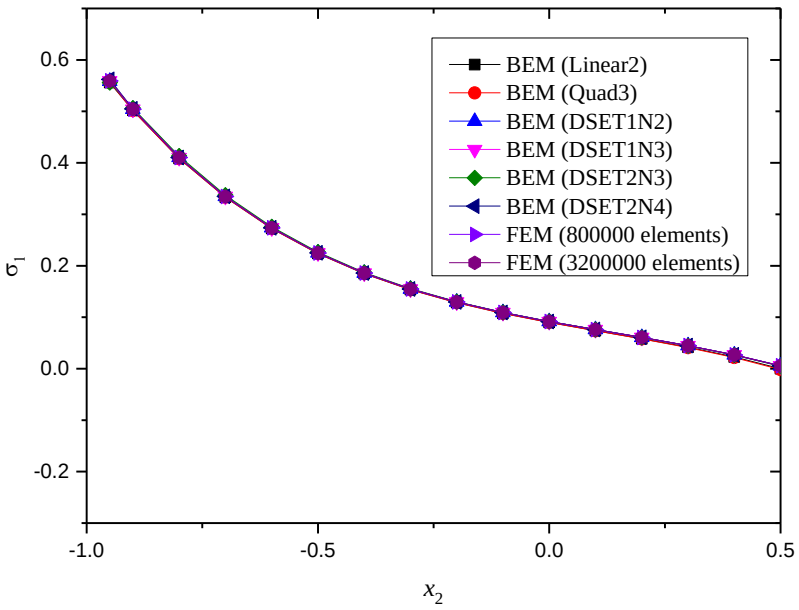

Figure 17. Stress σ_1 far from the concentrated load point

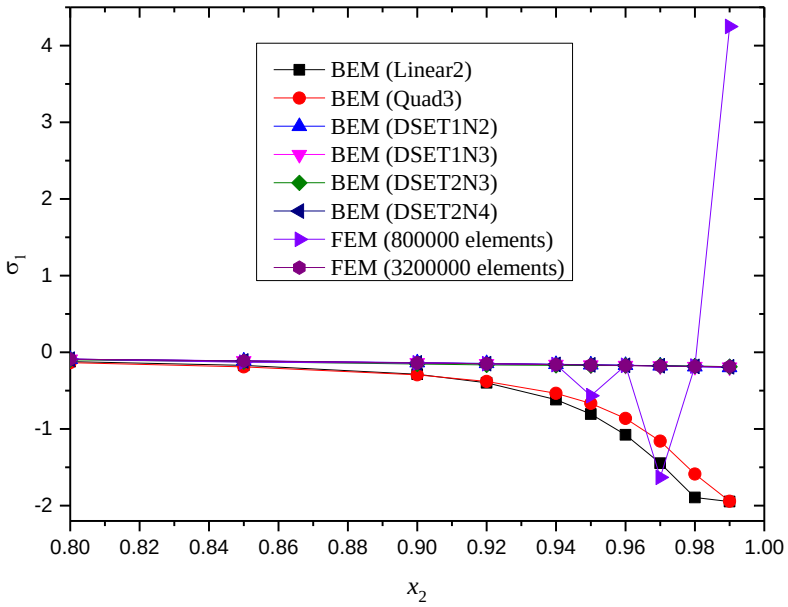

Figure 18. Stress σ_1 near the concentrated load point

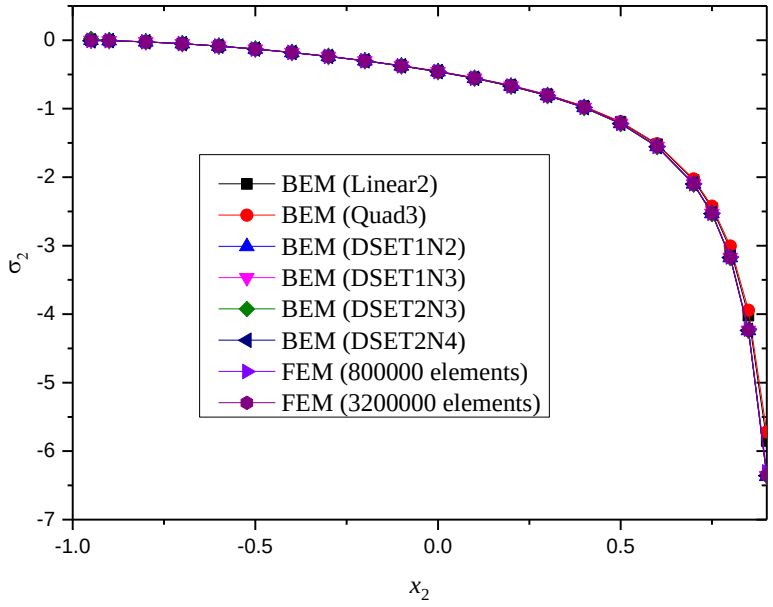

Figure 19. Stress σ_2 far from the concentrated load point

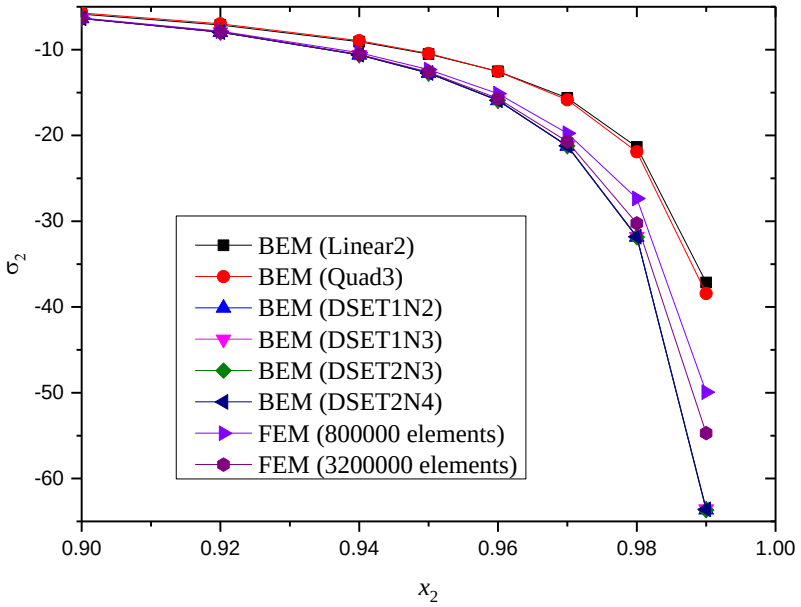

Figure 20. Stress σ_2 near the concentrated load point

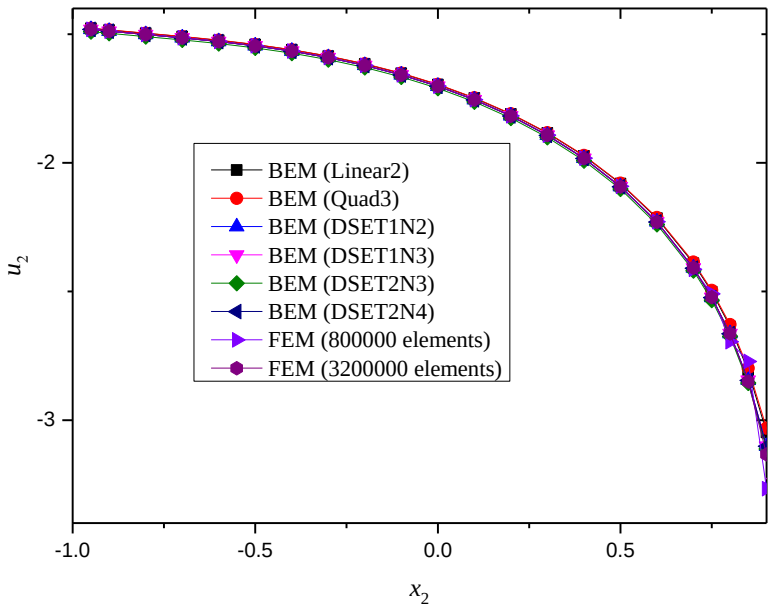

Figure 21. Displacement u_2 far from the concentrated load point

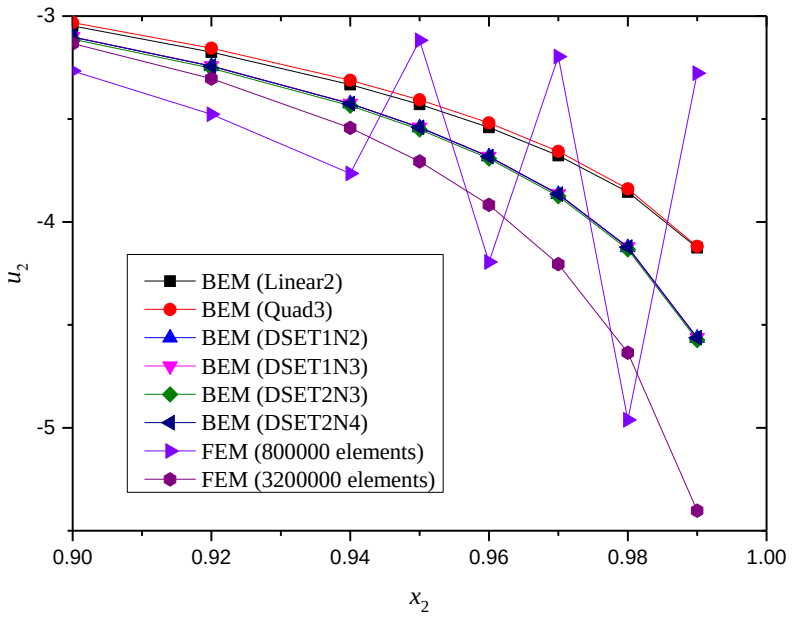

Figure 22. Displacement u_2 near the concentrated load point

6.4. A plate with void

A plate with a void at the center under pull and five concentrated loads is shown in Figure 23, where $L=20$, $R=1.0$, $P=1.0$ and $F=1.0$. Six types of elements applied in example 6.2 are also used to solve this problem by BEM, and 2,400 nodes are used to discretize the boundary.

FEM is also applied for purpose of comparison. The stress σ_1 on line $x_1 = 0$ is shown in Figures 24 and 25. The results obtained by BEM with Linear2, Quad3, DSET1N2, DSET1N3 and DSET2N4 are in good agreement with each other for all points on line $x_1 = 0$, however, the results obtained by FEM is much lower at points near the void. Figures 26 and 27 plot the stress σ_1 on line $x_2 = 0$, and a little difference can be observed at points near the void. However, the difference at points near the concentrated load point is very large, which can be observed from Figure 27. The stress obtained by BEM with displacement singular elements is much higher than it obtained by other methods, and the result of FEM is the lowest.

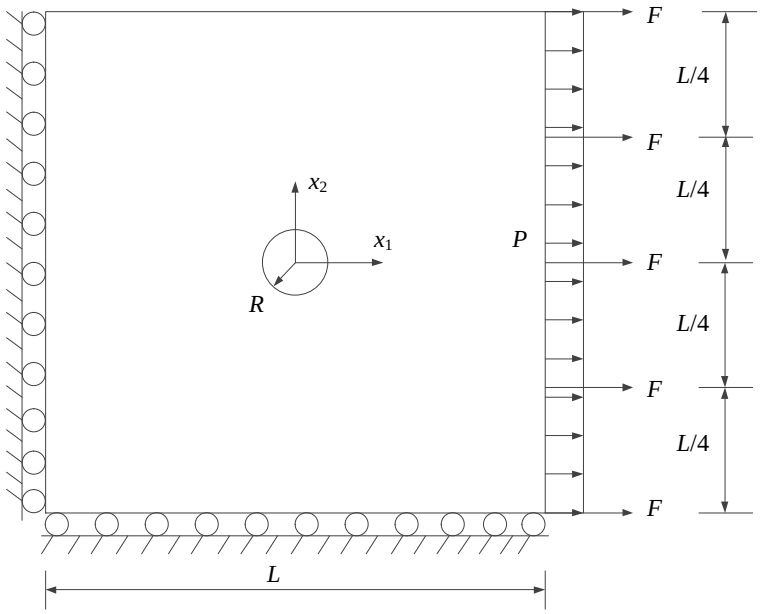

Figure 23. A plate with void

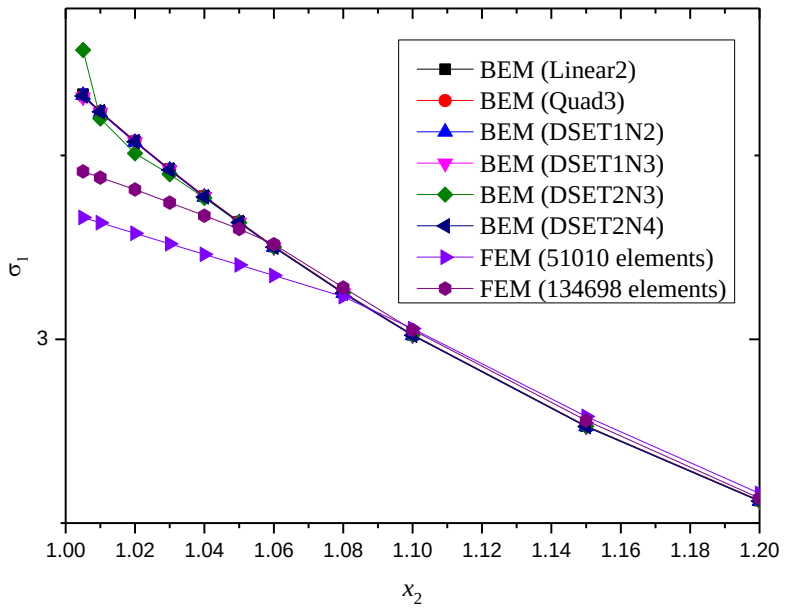

Figure 24. Stress σ_1 near the void

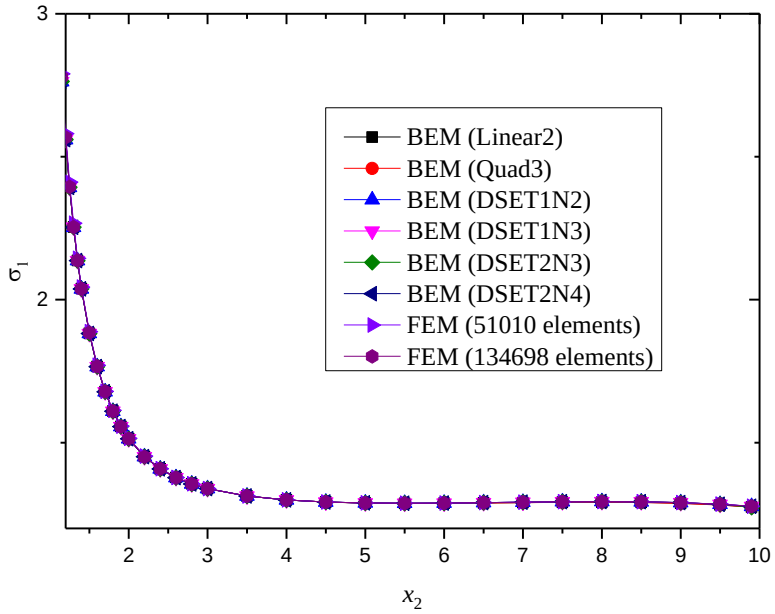

Figure 25. Stress σ_1 far from the void

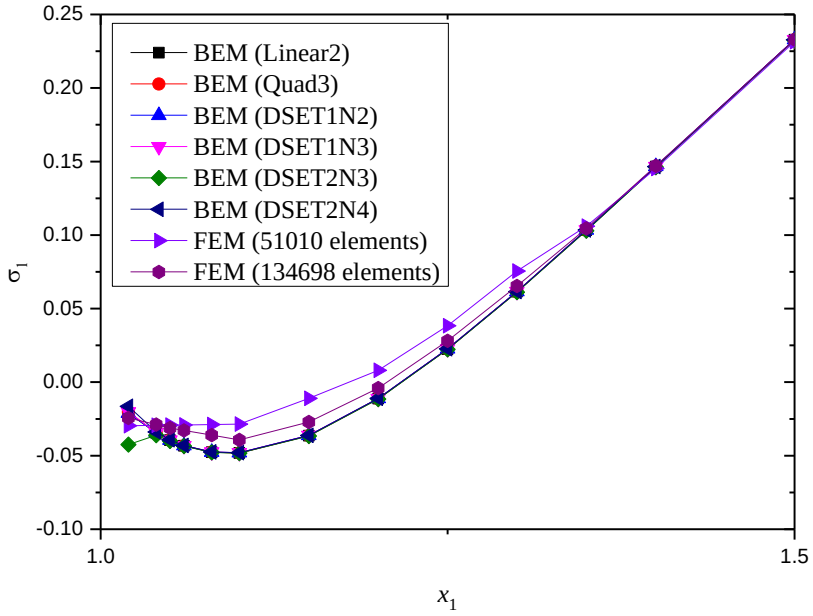

Figure 26. Stress σ_1 near the void

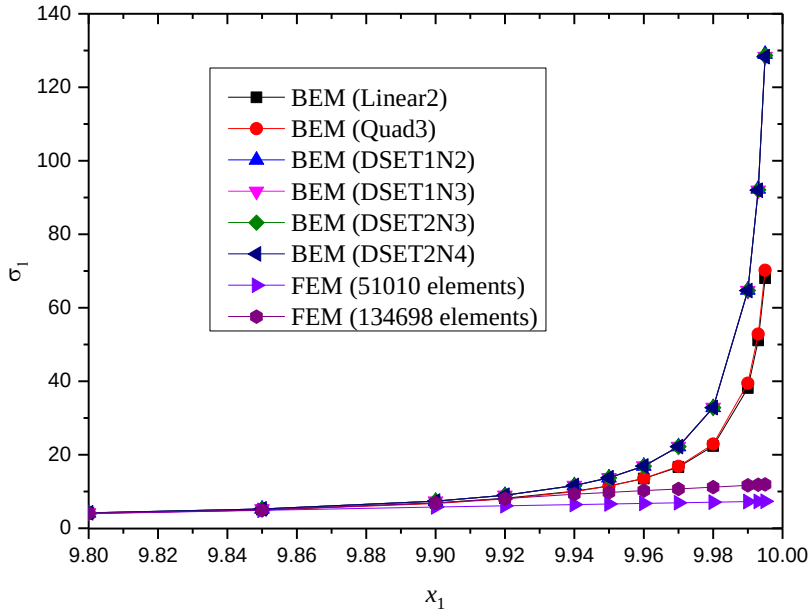

Figure 27. Stress σ_1 near the concentrated load point

7. Conclusion

The boundary element method for elasticity problems with concentrated loads is proposed. Two types of displacement singular elements are introduced to capture the singularities at

concentrated load points. No refinement mesh is needed near the concentrated load points and high accuracy can be observed compared with the traditional BEM and FEM. The element type DSET2 with two concentrated load points at the element edges is a general element type, which can also work well for problems without concentrated loads.

In the proposed displacement singular elements, an adaptive scheme is applied to compute the singular and nearly singular integrals. This procedure is time consuming and some more efficient methods [20-22] can be used to accelerate the integration.

The proposed methods can also be applied in other problems with singular loads, such as 3D elasticity problems with concentrated loads.

Acknowledgments

Financial support for the project from the National Key R&D Program of China (No. 2017YFC0404802) and National Natural Science Foundation of China (No. 51609181) is acknowledged.

References:

1. M. Jaswon, *Integral equation methods in potential theory. I.* Proceedings of the Royal Society of London. Series A. Mathematical and Physical Sciences, 1963. **275**(1360): p. 23-32.
2. M.A. Jaswon and G.T. Symm, *Integral equation methods in potential theory and elastostatics*. 1977, United Kingdom: Oxford Univ Press.
3. Z. Yao and H. Wang, *Some benchmark problems and basic ideas on the accuracy of boundary element analysis.* Engineering Analysis with Boundary Elements, 2013. **37**(12): p. 1674-1692.
4. Z. Yao, *A new type of high-accuracy BEM and local stress analysis of real beam, plate and shell structures.* Engineering Analysis with Boundary Elements, 2016. **65**: p. 1-17.
5. Z. Liu, J. Liang, Y. Huang, and L. Liu, *IBIEM modelling of the amplification of seismic waves by a three-dimensional layered alluvial basin.* Geophysical Journal International, 2015. **204**(2): p. 999-1023.
6. F. Tan and Y.-Y. Jiao, *The combination of the boundary element method and the numerical manifold method for potential problems.* Engineering Analysis with Boundary Elements, 2017. **74**: p. 19-23.
7. J. Zhang, L. Han, W. Lin, Y. Dong, and C. Ju, *A new implementation of BEM by an expanding element interpolation method.* Engineering Analysis with Boundary Elements, 2017. **78**: p. 1-7.
8. J. Zhang, W. Lin, Y. Dong, and C. Ju, *A double-layer interpolation method for implementation of BEM analysis of problems in potential theory.* Applied Mathematical Modelling, 2017. **51**: p. 250-269.
9. J. Zhang, Y. Dong, C. Ju, and W. Lin, *A new singular element for evaluating stress intensity*

factors of V-shaped notches under mixed-mode load. Engineering Analysis with Boundary Elements, 2018. **93**: p. 161-166.

10. Y. Gu, X. He, W. Chen, and C. Zhang, *Analysis of three-dimensional anisotropic heat conduction problems on thin domains using an advanced boundary element method.* Computers & Mathematics with Applications, 2018. **75**(1): p. 33-44.
11. H.-F. Peng, M. Cui, K. Yang, and X.-W. Gao, *Radial integration BEM for steady convection-conduction problem with spatially variable velocity and thermal conductivity.* International Journal of Heat and Mass Transfer, 2018. **126**: p. 1150-1161.
12. Y. Gu, C. Zhang, W. Qu, and J. Ding, *Investigation on near-boundary solutions for three-dimensional elasticity problems by an advanced BEM.* International Journal of Mechanical Sciences, 2018. **142-143**: p. 269-275.
13. J. Qian, *Boundary element method with concentrated force.* Engineering Mechanics, 1990. **7**(2): p. 140-144.
14. Z. Wang and Y. Wang, *Spline boundary element method for the analysis of elastic body subjected to concentrated forces.* Shanghai Jouranl of mechanics, 1994. **15**(1): p. 55-60.
15. Q. Wang, W. Zhou, Y. Cheng, G. Ma, X. Chang, and E. Chen, *NE-IIBEFM for problems with body forces: A seamless integration of the boundary type meshfree method and the NURBS boundary in CAD.* Advances in Engineering Software, 2018. **118**: p. 1-17.
16. J. Telles, *A self‐adaptive co‐ordinate transformation for efficient numerical evaluation of general boundary element integrals.* International Journal for Numerical Methods in Engineering, 1987. **24**(5): p. 959-973.
17. M. Guiggiani, G. Krishnasamy, T.J. Rudolphi, and F. Rizzo, *A general algorithm for the numerical solution of hypersingular boundary integral equations.* Journal of applied mechanics, 1992. **59**(3): p. 604-614.
18. M. Guiggiani, *Formulation and numerical treatment of boundary integral equations with hypersingular kernels.* Singular integrals in boundary element methods, 1998: p. 85-124.
19. Q. WANG, *SEVERAL SPECIAL DISPLACEMENT SOLUTIONS AND COMMENTS UNDER CONCENTRATED FORCE.* Chinese Journal of Rock Mechanics and Engineering, 2005. **24**(2): p. 5576-5579.
20. J. Lv, Y. Miao, W. Gong, and H. Zhu, *The sinh transformation for curved elements using the general distance function.* Comput Model Eng Sci, 2013. **93**(2): p. 113-131.
21. J.-H. Lv, X.-T. Feng, F. Yan, P.-Z. Pan, and G.-Z. Xie, *A combined conformal and sinh–sigmoidal transformations method for nearly singular boundary element integrals.* Engineering Analysis with Boundary Elements, 2015. **58**: p. 166-175.
22. Y. Miao, W. Li, J. Lv, and X. Long, *Distance transformation for the numerical evaluation of nearly singular integrals on triangular elements.* Engineering Analysis with Boundary Elements, 2013. **37**(10): p. 1311-1317.